Non-Data Aided Doppler Shift Estimation for Underwater Acoustic Communication

(Invited paper)

Paul Cotae (Corresponding author) [1,*], Suresh Regmi[1], Ira S. Moskowitz[2]

[1]University of the District of Columbia, Electrical and Computer Engineering, Washington DC, USA
[2] Naval Research Laboratory Centre for High Assurance Computer Systems, Code 5540, Washington, DC, USA
*Corresponding author (Email: pcotae@udc.edu)

Abstract— **In this paper, we investigated different methods for blind Doppler shift estimation and compensation for a single carrier in underwater acoustic wireless sensor networks. We analyzed the data collected from our experiments using non-data aided (blind) techniques such as Power Spectrum Analysis, Autocorrelation, and Squaring Time Phase Recovery methods in order to estimate the Doppler shift in collaborative distributed underwater sensor networks. Detailed experimental and simulated results based on second order cyclostationary features of the received signals are presented.**
Keywords: **Blind Doppler Shift Estimation, Underwater Communication, Autocorrelation, Power Spectral Density (PSD), Periodogram.**

I. INTRODUCTION

Doppler shift estimation and detection for target localization and tracking in underwater wireless communication (UWC) has been a major topic of research and investigation due to the increasing use of aquatic channels [2], [4], [12], and [15]. The need for Doppler shift estimation in UWC exists mostly for real time remote control monitoring of oceanic activities: environmental monitoring, scientific data collection, tracking, and locating objects.

There are several primary obstacles for reliable communication in underwater environment, including time-varying multipath, fading, low sound speed and noise. The sound speed underwater is about 1500 m/s. The low sound speed and relative high platform speed result in Doppler shifts several times those encountered in radio transmission [14]. The ratio of platform speed to sound propagation speed is large enough to cause time compression or expansion of the symbol pulse itself [4], [13]. The motion-induced pulse compression or expansion makes symbol synchronization of equal importance to carrier frequency identification, thus becoming a major constraint of mobile UWC. Current UWC methods are mostly used for low Doppler environment [4].

Due to complexities of the underwater channel, such as multi-path propagation, time variations, small available bandwidth and strong signal attenuation, (especially over long ranges) various factors of a communication system such as data rate, symbol synchronization, carrier phase recovery and the speed of propagation are compromised [3]. As a consequence, at the digital receiver end, different levels of synchronization: carrier recovery, frame synchronization, symbol and data bit timing recovery are strongly affected [9], [10] and [14]. Therefore, continuous time communications between rapidly moving platforms is the driver for new robust methods for blind synchronization (non-data aided) techniques able to track large and variable Doppler shifts.

In order to estimate and compensate for the Doppler shift, different coherent and blind methods have been implemented for pseudorandom sequence estimation. The most popular can be categorized as eigenanalysis based on subspace methods, and exploiting the spectral characteristics in cyclostationarity signals. In [2], [4] it has been proven that the spectral characteristics of cyclostationarity signals is computationally less complex and more robust for pseudorandom (PN) sequence estimation then subspace methods. Therefore, we have chosen the experimental approach to estimate the Doppler shift using blind spectral estimation methods for data modulated by PN sequences.

In [11], spectral correlation based signal detection has been proposed. The spectral correlation theory in [11] is used to calculate spectral correlation function and it could be used for Doppler shift estimation. However, in this method, the received baseband signal is no longer orthogonal to the transmitted *m*-sequences. As a result, in the frequency domain, it is very hard to read the instantaneous Doppler shift due to fading.

In [6] the concept of passive signal detection is carried forward to active signal detection using a Dopplergram and an ambiguity function has been used to determine Doppler shift for *m*-sequence modulation. However, in both [6] and [11], only one method of modulation (*m*-sequence modulation technique) has been used. In addition, in [4], the spectral correlation function is modified to the spectrum coherence function to estimate carrier frequency and symbol rate estimation. It was assumed that in underwater communication, channel characteristics vary quickly and the signal parameters vary quickly as well.

In this paper, we conducted experiments for underwater acoustic wireless communication using a pair of SAM-1

978-1-4799-2385-4/14/$31.00

sensors provided by Desert Star Systems. We used universal asynchronous receiver transmitter protocol for serial data communication. MATLAB software was used to send data via the serial port for transmission and acquire data from a sensor into a personal computer (PC). We analyzed the data collected from our experiments using non-data aided techniques such as Power Spectrum analysis, Autocorrelation and Squaring Time Phase Recovery (Oerder & Meyr) [1] methods in order to estimate Doppler shift in collaborative distributed underwater sensor networks. In our study, the sensors were half-duplex, and therefore could only transmit or receive at a given time.

We improved the MATLAB code for serial data communication for acoustic sensors (SAM-1) provided by Desert Star Systems. We transmitted original and modulated 52 *m*-sequences each of length 1023 bits, via sensors in an acoustic prototype environment and at the receiver end we analyzed the received signal using spectral analysis and the Oerder and Meyr method. The size of the baseband transmitted covariance matrix is 106392x106392. The received signal correlation matrix is 1x106392 for the original *m*-sequences.

The rest of the paper is organized as follows: In Section II we describe the theoretical background, Section III presents the experimental model, Section IV contains our simulated and experimental results. Conclusion and acknowledgements are drawn in section V.

II. Theoretical Background

1) Doppler Effect

Generally, change in the frequency of an emitted wave caused by the motion of an emitted source relative to observer or vice versa is defined as Doppler shift or effect. For a communication system, the received signal at the receiver end can be characterized as:

$$r(t) = \Re\{\sum_{n=-\infty}^{+\infty} d_n\, g(t-nT)\, e^{j2\pi f_c t}\} + n(t) \qquad (1)$$

where, $\Re$ represents real part of signal, $n(t)$ is the AWGN with zero mean circular complex white Gaussian process statistically independent signal, f_c is the carrier frequency, d_n is the transmitted data symbol in the time interval $nT \le t \le (n+1)T$, T is data symbol duration and, $g(t)$ is the convolution product of impulse response of pulse shaping filter g_E(t), channel impulse response $h(t)$, and receiver filter impulse response $g_R\,(t)$ [12].

In wide band cases, due to the Doppler effect, signal carrier frequency suffers frequency scaling $f_c(1-\delta_d)$ and the received baseband signal undergoes time scaling $t(1-\delta_d)$, so the received signal at the receiver input is given in [2] and [16] as:

$$r(t) = \Re\{\sum_{n=-\infty}^{+\infty} d_n\, g(t(1-\delta_d)-nT)e^{j2\pi f_c(1-\delta_d)t}\} + n(t) \qquad (2)$$

where δ_d is the relative Doppler shift. This relation is valid for both wireless communication systems and UWC systems. But, the Doppler shift in underwater communication is very high. For underwater communication with multipath and fading, the received signal can be given as:

$$r(t,\delta_d) = \Re\{\sum_{l=0}^{L-1}\sum_{n=-\infty}^{+\infty} A_l(t)e^{j\theta_l(t)} d_n g[t(1-\delta_d) - -nT]e^{j2\pi[f_c+\Delta f]t(1-\delta_d)}\} + n(t) \qquad (3)$$

where $A_l(t)$ is the fading gain of l^{th} path, L is the number of multipath component, and $\theta_l(t)$ is the phase offset due to the channel on l^{th} path.

Different coherent techniques have been used to estimate Doppler shift but the proposed algorithms used to find cyclic frequency offset are more susceptible to ISI (Inter Symbol Interference). Thus, non-coherent techniques are preferred to find cyclic frequency offset and Doppler compensation [7], [8], [16] and [17].

2) Spectral Analysis

Most random processes encountered in nature arise from some periodic phenomena. The random processes generated from such periodic phenomena produces data that are not periodic functions of time, but their statistical properties varies with time. These kinds of random processes are modeled as wide-sense cyclostationarity random processes and its features can be used in signal detection and estimation. Therefore random processes in this paper are considered to be cyclostationary.

Cyclostationary analysis is based on the fact that communications signals are not accurately described as stationary, but rather more appropriately modeled as cyclostationary. While stationary signals have statistics that remain constant in time, the statistics of cyclostationary signals vary periodically. These periodicities occur for signals of interest in well-defined manners due to underlying periodicities such as sampling, modulating, multiplexing, and coding.

A process, say $x(t)$, is said to be wide sense cyclostationary if it's mean ($E\{x(t)\}$) and autocorrelation function ($R_x(t,\tau)$) are periodic with the same period T:

$$E\{x(t+T)\} = E\{x(t)\} \qquad (4)$$

$$R_x(t+T,\tau) = R_x(t,\tau) \qquad (5)$$

In [7], the Fourier series expansion of this periodic autocorrelation function converges. As in [14], (5) can be expressed as:

$$R_x(t,\tau) = \sum_{n=-\infty}^{+\infty} R_x^{\frac{n}{T}}(\tau) e^{j2\pi\left(\frac{n}{T}\right)t} \qquad (6)$$

where $\frac{n}{T} = \alpha$ is called the cyclic frequency; $R_x^{\frac{n}{T}}(\tau)$ is the cyclic autocorrelation function at cyclic frequency α and is given as follows:

$$R_x^{\alpha}(\tau) \triangleq \lim_{T\to\infty} \frac{1}{T}\int_{-T/2}^{T/2} R_x(t,\tau)e^{-j2\pi\alpha t}\,dt \qquad (7)$$

Now for random process, the Fourier transform of the autocorrelation will give the Power Spectral Density (PSD) and (7) can be expressed in so called cyclic power spectral density as:

$$S_x^{\alpha}(f) = \sum_{\tau=-\infty}^{+\infty} R_x^{\alpha}(\tau)e^{-j2\pi f\tau} \qquad (8)$$

The cyclic PSD, $S_x^{\alpha}(f)$, contains spectral discrete components which are useful to estimate the Doppler shift for different modulated signals.

Furthermore, spectral components, $S_x^{\alpha}(f)$, of signal $x(t)$ are the measurement of cyclic power spectral density which can be more elaborated by the normalized correlation between two spectral components of $x(t)$ at $f+\frac{\alpha}{2}$ and $f-\frac{\alpha}{2}$ frequencies over an interval of Δt. Then the ideal measurements can be mathematically expressed as in [14]:

$$S_x^{\alpha}(f) = \lim_{T\to\infty}\lim_{\Delta t\to\infty}\frac{1}{\Delta t}\int_{-\frac{\Delta t}{2}}^{\frac{\Delta t}{2}}\frac{1}{T}x_T(t,\ f+\tfrac{\alpha}{2})x_T^*\left(t, f-\tfrac{\alpha}{2}\right)dt \qquad (9)$$

where the finite time Fourier transform of $x(t)$ over time interval $t+\frac{T}{2}$ and $t-\frac{T}{2}$ is:

$$X_T(t,f) = \int_{t-T/2}^{t+T/2} x(u)e^{j2\pi fu}du \qquad (10)$$

III. Experimental Model

We conducted experiments in an indoor water tank, and in an indoor swimming pool. The tank was 7x5x2.5 ft^3 in volume. The data were transferred using a pair of acoustic modems and were processed in MATLAB. Also we used a hydrophone to measure sound underwater and an acoustic speaker to generate noise. Fig. 1 illustrates our prototype environment; where the sensors are connected to the computer via a serial port and are floating in the water.

In the swimming pool, distance between two communicating sensors was 15 yards and the depth of the swimming pool was 11ft and 8 inches. The surface temperature of the swimming pool was 70^0 Fahrenheit and the water was chlorinated.

IV. Experimental Results

Our experiment is based on serial data transfer. The data was transmitted at 4800 baud and 8 data bits. We measured the noise during our experiment for the length of 3.65 minutes sampled at the rate of .01s and we plotted its PSD.

From Fig. 2 one can notice that the power of noise is high for frequency range of 0 to 5 kHz. As the frequency increases we observe that the power of noise is less than $-11.11.86$ dB. If we are able to transmit the signal in the frequency range where the noise power is relatively less, we can obtain better performance. Therefore, we have chosen 17 kHz of carrier frequency for our experiments. We could use any frequencies above 5 kHz and below 40 kHz, but to be consistent with results presented in [2], [4], we preferred 17 kHz.

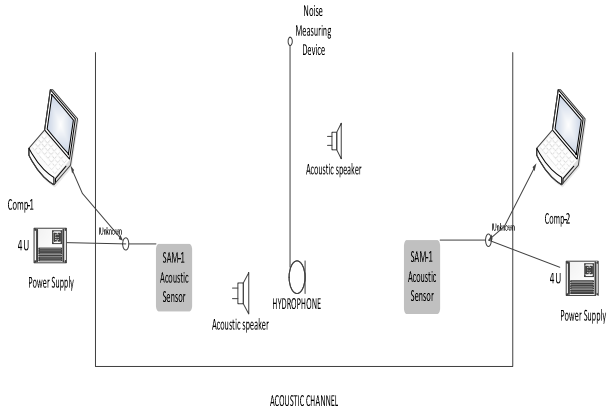

Figure 1 Experimental set up and its components

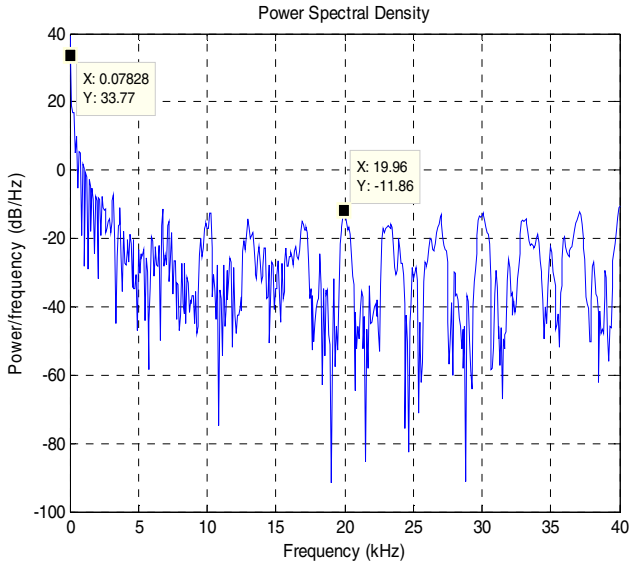

Figure 2 PSD of measured noise in swimming pool

In our experiments the transmitted signal had a carrier frequency of 17 kHz and a sampling rate of 8000 samples/sec. The transmitted spectrum in both the cases (tank and pool) had almost a flat spectrum. For the 1st case the transmitted signal is a PN sequence of length 1023 bits modulated by a carrier of 17 kHz. We plotted the autocorrelation and partial PSD of the received signal and observed the different spectral components to estimate Doppler shift for both tank and pool.

It is clear form Fig. 3 that based on the autocorrelation function of the received signal we were able to distinguish

the transmitted 52 m-sequences. However, the received signal is not free of noise and some multipath components. The dark lines on Fig .3 refer to the cross-spectral correlation effect. The bold dense line on the autocorrelation of the transmitted signal is due to modulation effect. We plotted the partial autocorrelation of the received signal and find out the transmitted m-sequences associated with it as in Fig. 4.

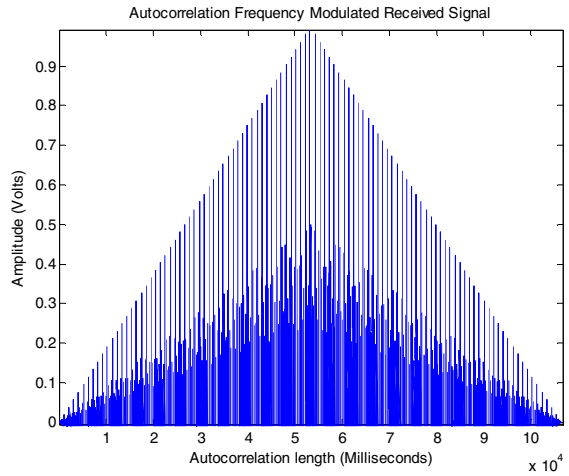

Figure 3 Autocorrelation function of the received 52 m -sequences

In Figure 4, we noticed that the time length difference between each m-sequence peak is not 1023 bits (in the transmitted signal it was exactly 1023 bits). Form this observation we concluded that the multipath effect must have affected the received signal during the period of 1023 milliseconds.

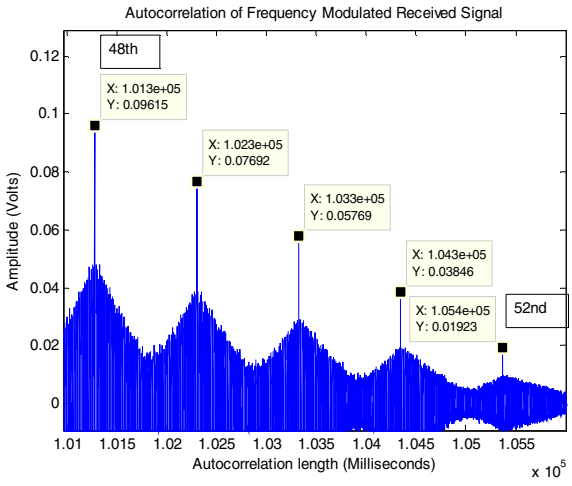

Figure 4 Partial autocorrelation of received signals showing 48th to 52nd m-sequences

In the case of the water tank experiment, we were able to receive same data that were sent with a bit error rate of 0.0078. Looking at the partial PSD around the carrier frequency and its period, in Fig. 5, we find the Doppler shift. The Doppler shift was 50 Hz at $f_c = 17$kHz. The partial PSD spectrum in Figure 6 shows that the Doppler shift is 20 Hz at $2f_c$. Taking average we conclude that the estimated Doppler shift is approximately 35 Hz.

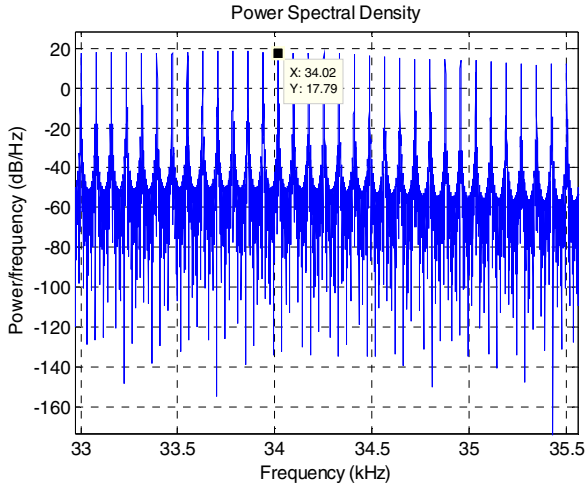

Figure 5 Partial PSD of a received signal around twice the carrier frequency (results for water tank)

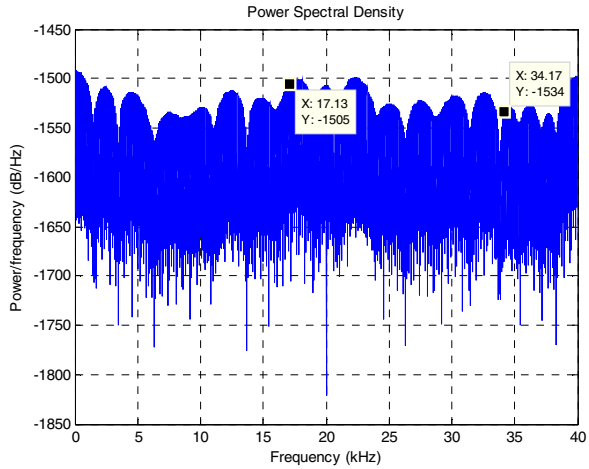

Figure 6 PSD of received signal (results for swimming pool)

After measuring the Doppler shift in the water tank, we performed experiments in the swimming pool. In the swimming pool, the transmission range was longer (25 yards) and the environment is echoic, so we experienced more of multipath effect. We searched for the local maxima around the carrier and found the Doppler shift to be 130 Hz at $f_c = 17$khz and 170Hz at $2f_c$ in average 150Hz. Then, we transmitted the Linear Frequency Modulated m-sequences signal and analyzed the signal using Oerder & Meyr squaring recovery circuit. Figures 7-8 show the partial PSD, and phase shift.

From Fig. 8, we see that average Doppler shift is 0.85 and the instantaneous shift of range [0-2.86]. From the experiments, we claim that Doppler shift could be

minimized by using double modulation technique instead of using either the LFM or m-sequence technique separately. This can be validated by the minimal shift obtained in Figure 8.

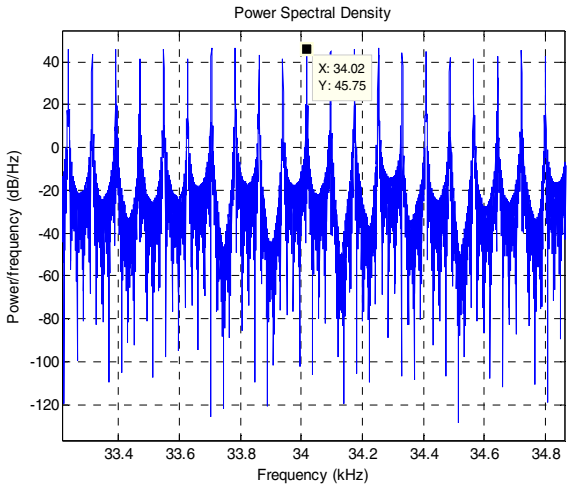

Figure 7 Partial PSD of LFM 52- *m*- sequences at 2nd period (34 kHz)

It can be observed that, for the proposed double modulation technique, phase shift is less than the one provided in [2]. The results provided in [2] were for m-sequence modulation and the average phase shift was 1.12 for the same parameters (k=100 symbols). From Fig. 8, we see that average Doppler shift is 0.85 and the instantaneous shift of range [0-2.86].

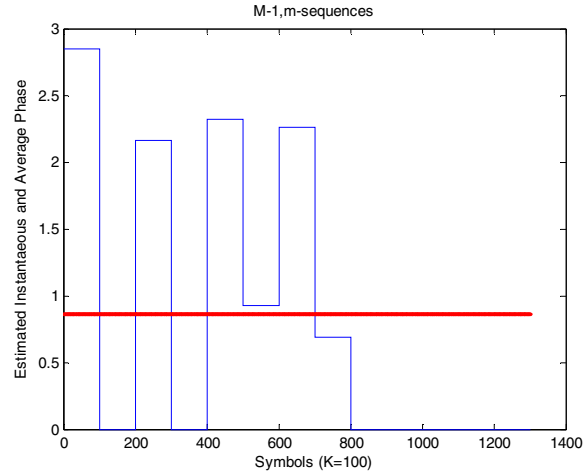

Figure 8 Estimation of Instantaneous and average Doppler shift using the Oerder & Meyr Algorithm

In Fig. 9 we focused only on the instantaneous estimated Doppler shift. The sampling frequency is 20Kz and the number of samples per symbols is 4: please see [17] and [18]. We converted the received baseband signal in a number of total 212784 samples and we used the same number of K=100 symbols per frame. Because we are using a blind method, we cannot compensate the Doppler shift for the first *m*-sequence and we obtained a "coarse" estimation of this.

We varied the numbers of symbols per frame between 50 and 100 symbols, and the results are not significantly changed. One possible explanation for this is that the number of samples per symbols is the same (=4), and from information theoretic point of view, the information extracted from each *m*-sequence is the same.

It is an interesting question to ask, what could be the optimum number of symbol per frame and the minimum number of samples per symbol, in order to get the optimum of performances or to get the maximum of information. This is left for future research and the results obtained in Fig.8 and Fig. 9 are a good start.

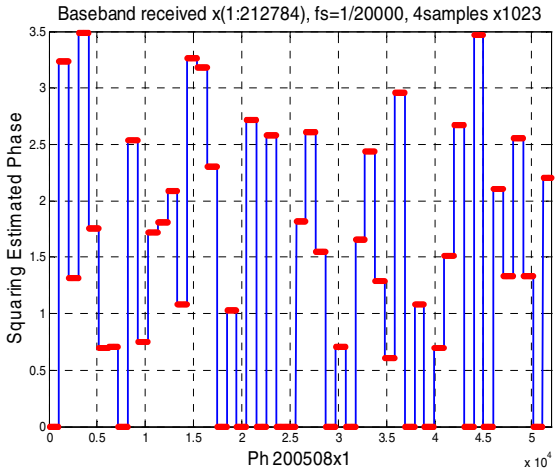

Figure 9 Instantaneous estimation of Doppler shift

We searched for a Doppler shift between [-30, 30] Hz and we wanted to plot all 52-ambiguity functions for each *m*-sequence as in Fig.11. Please note a scale change for Doppler shift measurement in Fig.10. In searching for the local maxima or minima of the ambiguity functions, we scaled the domain of definition for these functions.

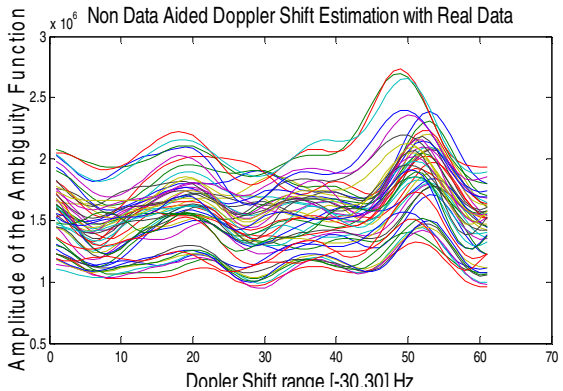

Fig. 10 The ambiguity function for all 52 m-sequences

In comparing with the method given in [2], in average, there is a difference of 0.5 Hz, and each *m*-sequence has a different Doppler shift. The explanation for this is the fact

that blind method is not a coherent one (data aided) and it depends which sample (out of four per symbol) is coming and processed first.

The best comparison is made directly on the Dopplergram [5] represented in Fig.11. From user perspective (Dopplergram) there is practically no difference between results in Fig.10 and that those presented in [5]. The explanation for this are the results presented in the Fig. 10, if we are looking only at the maximum of the ambiguity functions. Based on Fig.10 we can provide directly the Dopplergram:

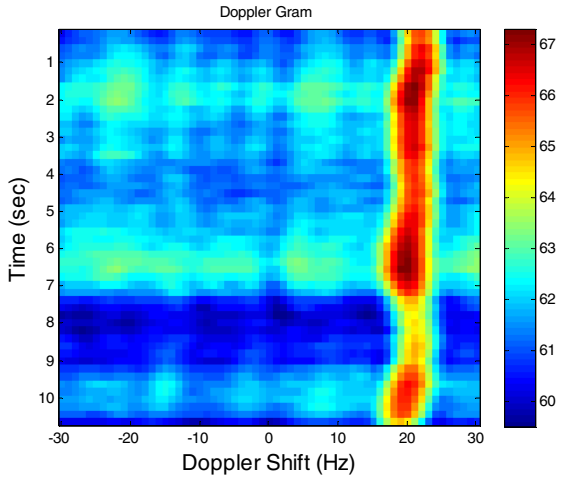

Figure 11 Dopplergram results

During our experiment we had several issues with data and software compatibility. Debugging was the most cumbersome part. It took several hours to run the MATLAB programs. Memory buffer size of sensors was another one challenging issue. We had problems with the sensors because they transmitted some random signals by themselves due to unknown internal error.

V. CONCLUSIONS

In this paper, we performed experiments in two different types of environment and studied the non-data aided techniques for Doppler shift estimation in underwater communication. We found that the Doppler shift for the large transmission range was higher than for the lower transmission range. We found that double modulation technique (combine LFM and *m*-sequence for modulation message signal) could minimize the phase shift even better than the modulation technique used in [3], for underwater communication.

Based on our observations, we conclude that the exploiting second order cyclostationary features of the received signal makes it easier and faster to estimate Doppler shift without prior knowledge of the signal transmitted. It is also concluded form our experiments that the proposed methods were very easy to implement.

ACKNOWLEDGMENT

The first two authors thank for the support from the DoD Grant W911NE-11-1-0144 and thank Dr. T.C. Yang for previous discussions and the research environment provided at NRL in Washington DC.

REFERENCES

[1] M., Oerder, and M., Heinrich "Digital Filter and Square Timing Recovery" IEEE Transaction on Communication, vol. COM-36, pp. 605-612, May 1988.

[2] P. Cotae and T. C. Yang. "A cyclostationary blind Doppler estimation method for underwater acoustic communications using direct-sequence spread spectrum signals." IEEE Proceedings of the 8th International Conference COMMUNICATION 2010, Bucharest, Romania, pp. 323-326, Jun. 2010.

[3] J.G. Proakis, and M. Salehi, Digital Communication, 5th ed. McGraw-Hill, 2008.

[4] Z. Wu and T.C Yang. "Blind Cyclostationary Carrier Frequency and Symbol Rate Estimation for Underwater Acoustic Communication." IEEE International Conference on Communication, pp. 2482-3486, June 2012.

[5] T.C., Yang "Acoustic Dopplergram for Intruder Defense." IEEE Ocean 2007, pp. 1-5.

[6] W. A. Gardner, A. Napolitano, and L. Paura, "Cyclostationary: Half a century of research" Signal processing Vol. 86, no.4, pp.639-697, 2006.

[7] W. A. Gardner, Introduction to Random processes with applications to signals and systems, New York: Macmilan, 1985.

[8] W. A. Gardner, "Exploitation of Spectral Redundancy in Cyclostationary Signals." IEEE Signal Processing Magazine, vol. 8, pp.14 - 37, 1991.

[9] Haykin, Simon. Adaptive Filter Theory. 3rd edition, Prentice Hall 1995.

[10] R. L. Peterson, R. E. Ziemer, and David E. Borth. Introduction to spread - spectrum communications, New Jersey: Prentice Hall, 1995.

[11] Han, Ning, et al. "Spectral correlation based signal detection method for spectrum sensing in IEEE 802.22 WRAN systems." Advanced Communication Technology, 2006. ICACT 2006. The 8th International Conference.Vol.3.IEEE,2006.

[12] R. Suresh "Non-Data Aided Doppler shift Estimation and Detection for Underwater Moving Targets - A Practical Approach" M.S Thesis, Dept.of Electrical and Computer Engineering, University of the District of Columbia, Washington D.C., May 2013.

[13] J.L. Seung and N.C. Beaulieu, "Performance Improvement of Non-Data-Aided Feedforward Symbol Timing Estimation Using the Better Than Raised-Cosine Pulse", IEEE Transactions on Communications, Vol. 56, Issue: 4, pp. 542 – 544, April 2008.

[14] Z. Ruolin, Xue Li, T.C. Yang, L. Zhiqiang and W. Zhiqiang "Real-time cyclostationary analysis for cognitive radio via software defined radio", IEEE Global Communications Conference (GLOBECOM), pp.1495 – 1500, 2012.

[15] H. Chengbing, H. Jianguo, Z. Qunfei and L.Kaizhuo"Reliable Mobile Underwater Wireless Communication Using Wideband Chirp Signal", International Conference on, Communications and Mobile Computing, 2009. CMC '09, Volume: 1, pp.146 - 150 ,Jan. 2009 .

[16] T, Jun, Y.R. Zheng, X. Chengshan, T.C. Yang and Wen-Bin Yang "Channel Estimation, Equalization and Phase Correction for Single Carrier Underwater Acoustic Communications", OCEANS 2008 - MTS/IEEE Kobe Techno-Ocean, pp 1 - 6 , 2008.

[17]F. M. Gardner, "A BPSK/QPSK timing-error detector for sampled receivers," IEEE Trans. Commun., vol. COM-34, no. 5, pp. 423–429, May 1986.

[18] K. Rajawat and A. K. Chaturvedi, "A low complexity symbol timing estimator for MIMO systems using two samples per symbol," IEEE Commun. Lett., vol. 10, no. 7, pp. 525–527, July 2006.